Telomere shortening in rat hepatic stem-like epithelial cells and subcellular localization of rat PinX1

Chan Hee Lee

Department of Medical Science

The Graduate School, Yonsei University

Telomere shortening in rat hepatic stem-like epithelial cells and subcellular localization of rat PinX1

Directed by Professor Young Nyun Park

The Master's Thesis
submitted to the Department of Medical Science,
the Graduate School of Yonsei University
in partial fulfillment of the requirements
for the degree of Master of Medical Science

Chan Hee Lee

December 2004

This certifies that the Master's Thesis of Chan Hee Lee is approved.

_____

Thesis Supervisor : Young Nyun Park

_____

Bong Kyeong Oh

_____

Jeon Han Park

The Graduate School
Yonsei University

December 2004

ACKNOWLEDGEMENTS

본 논문을 완성함에 있어서 세심한 지도와 깊은 관심으로 이끌어 주신 박영년 교수님께 진심으로 감사 드립니다. 또한 진정한 과학자의 본을 가르쳐 주신 오봉경 교수님께도 진심으로 감사 드립니다. 그리고 좋은 조언으로 논문을 심사해 주신 박전한 교수님께 감사를 드립니다. 항상 따뜻한 관심으로 배려해주신 김건홍 선생님, 송택선 선생님, 전성후 선생님께도 감사의 말씀을 드립니다. 또한 병리학교실이라는 울타리 안의 모든 분들께도 감사 드리고 싶습니다. 오랜 벗 영주에게도 고마움을 전하며 함께 있어 소중한 친구 태선, 여식, 현석에게는 변치 않는 믿음으로 고마움을 대신할까 합니다. 2년여 동안의 대학원 생활이 쉽지만은 않았지만 따뜻한 관심을 가져주신 주변 분들이 계셨기에 지금의 제가 있을 수 있었습니다. 사랑하는 도희, 나희에게도 고마움을 전하며, 마지막으로 한결 같은 믿음으로써 저를 사랑해주신 어머니께 감사의 마음을 담아 이 논문을 드립니다.

저자 씀

Table of Contents

LIST OF FIGURES

ABSTRACT

Telomere shortening in rat hepatic stem-like epithelial cells and subcellular localization of rat PinX1

Chan Hee Lee

Department of Medical Science

The Graduate School, Yonsei University

(Directed by Professor Young Nyun Park)

Rat hepatic stem-like epithelial cells, LE/2, LE/6 and WB-F344, share a number of phenotypic properties with oval cells which are able to be observed in the early stages of hepatocarcinogenesis. Telomerase, a ribonucleoprotein complex, prevents telomeric shortening by adding TTAGGG repeats to the 3' end of telomeres, therefore the activation of this enzyme is required for cells to overcome replicative senescence and obtain the ability to divide without limits. In the previous study, the telomerase activity of LE/2, LE/6 and WB-F344 cells declined from the early to intermediate passages, and progressively increased from the intermediate to late passages. At the late passages, the activity reached up to higher level than the initial level. To know the telomere maintainance of these telomerase positive cell lines, telomere length was

measured during *in vitro* aging. These cells displayed no apparent aging phenotypes for over 140 passages, and telomere length of these cells progressively decreased with the passages. At the late passages, telomere shortening appeared to be reduced as telomerase activity increased. The relationship between telomere length and telomerase activity suggests that telomerase contributes to the regulation of telomere length in these cells. Short telomeres is known to result in hypersensitivity to ionizing radiation in mouse. To investigate whether shortened telomere of these rat epithelial cells is sensitive to ionizing radiation, γ-ray was irradiated to LE/2, LE/6 and WB-F344 cells in different passages. There was no significant difference of cellular sensitivity to γ-irradiation according to the different passages. This result suggests that the telomere length in these cells might not be critically shortened to induce chromosomal instability. Recently, PinX1 was identified from human and *Saccharomyces cerevisiae* as a potent telomerase inhibitor, however its function is not clearly understood. To confirm PinX1 localization in rodent, which has different features of telomerase and telomere length from human, PinX1 gene was cloned from WB-F344 cell line and then overexpressed in NIH/3T3 cells. Confocal microscopy showed that rPinX1 localized exclusively to the nucleolus, while rPinX1 Δ N, N-terminus 257 amino acids deleted form, was found in the nucleus and the cytoplasm. Taken together, subsequent telomere shortening at the late passage was reduced by reactivated telomerase activity. And the subcellular localization of PinX1 may contribute to its function on telomerase inhibition.

Key words : Rat hepatic stem-like epithelial cell, telomerase, telomere, PinX1, γ-irradiation

Telomere shortening in rat hepatic stem-like epithelial cells and subcellular localization of rat PinX1

Chan Hee Lee

Department of Medical Science
The Graduate School, Yonsei University

(Directed by Professor Young Nyun Park)

I. INTRODUCTION

Several hepatic stem-like epithelial cells have been isolated from rat liver. LE/2 and LE/6 were derived from rat maintained on a choline-deficient carcinogenic diet for 2 weeks and 6 weeks, respectively,[1] and WB-F344 cell line was established from normal rat liver.[2,3] These cell lines share a number of phenotypic properties with oval cells, which are observed in the early stages of hepatocarcinogenesis induced by chemical carcinogens.[4,5] Mammalian telomeres are composed of TTAGGG repeat and associated with specific DNA-binding proteins.[6,7] Telomeres cap the ends of the chromosome, forming a higher-order chromatin structure that protects the end from degradation and end-to-end fusions.[8] Telomerase, a ribonucleoprotein DNA polymerase, is composed of RNA and a catalytic protein subunit, called TR

and TERT, respectively,[9,10] and several associating proteins.[11] Human normal somatic cells are known to have undetectable level of telomerase activity, which results in loss of telomeres from the end with an average of 50~200 bp during each cell division.[12,13] When the telomeres reach a critically short length, cells stop dividing and enter senescence.[13,14] However, the cells bypassed cellular senescence by transfection with oncogenes such as SV40 large T antigen have detectable telomerase activity and stabilized telomeres.[13] Telomerase is also detected in most human malignant tissues but not in surrounding non-tumorous tissues.[15,16] These results suggest an importance of telomerase reactivation for human cell immortalization.

In contrast to human cells, rodent somatic cells constitutively express the telomerase activity and possess long telomeres ranging from 20 to 150 kb,[17,18,19,20] and undergo immortalization in culture spontaneously.[21] Moreover, malignant mouse cells maintain long telomeres.[20] Therefore, it has been suggested that telomere shortening and telomerase activation may contribute little to cellular senescence, immortalization or tumorigenesis in the rodent cells.[21]

Ionizing radiation (IR), a potent inducer of DNA double strand breaks (D SBs) on chromosomes, can threat the cell because DSBs disrupt the integrity of genome. Short telomeres are reported to enhance IR-induced lethality in telomerase deficient mice.[22,23] In addition, cells from organisms with defects in telomere maintenance are frequently radiosensitive.[24,25,26] How the telomere length involves in sensitivity to IR, however, is not understood.

Recently, PinX1 was identified as a telomerase inhibitor in human cells[27,28] and its telomerase inhibitory domain (TID), consisting of amino acids +254-328, almost completely inhibit telomerase activiy.[10] PinX1 directly

binds to the hTERT and hTR[29] and the telomere binding protein hTRF1.[28] PinX1 contains glycine rich domain (G-patch) at the N-terminus, known to be a RNA binding motif.[10] In the budding yeast, overexpression of the PinX1 lead to telomere shortening and telomerase inhibition,[30] and the PinX1 protein was found in nucleolus fraction.[31]

We studied *in vitro* aging of rat hepatic stem-like epithelial cells with the LE/2 and LE/6 cell lines, and compared them with the WB-F344 cell line in regard to the proliferation rate, telomere length and radiosensitivity. In addition, we confirmed the localization of PinX1 in rodent by cloning PinX1 from WB-F344, and analyzed its subcellular localization was analysed.

II. MATERIALS AND METHODS

1. Cell culture

LE/2, LE/6 and WB-F344 at the early passages were kindly provided by Dr. N. Fausto's lab and Dr. J.W. Grisham's lab, respectively. NIH/3T3, mouse embryo fibroblast, purchased from Korean Cell Line Bank. NIH/3T3 cells were maintained in RPMI 1640 (Invitrogen, Carlsbad, CA, USA) with 10% (vol/vol) fetal bovine serum (FBS), penicillin (100 unit/㎖), and streptomycin (100 ㎍/㎖). LE/2 and LE/6 were maintained in a 1:1 mix of DMEM (high glucose) (Invitrogen) and Ham's F10 supplement (Invitrogen) with 10% FBS (Invitrogen), insulin (final concentration 1 ㎍/㎖) (Sigma, St. louis, MO, USA), hydrocortisone (0.5 ㎍/㎖) (Sigma) and gentamicin (10 ㎍/㎖) (Invitrogen). WB-F344 cells were maintained in F12/DMEM supplemented with 10% (vol/vol) FBS, penicillin (100 units/㎖), and streptomycin (100 ㎍/㎖). All culture incubations were performed in a humidified 37℃, 5% CO_2 incubator. Cells grown at 80-90% confluency in a 100-mm tissue culture dish (NUNC™, Rochester, NY, USA) were washed twice with 5 ㎖ PBS without Ca^{2+} and Mg^{2+} and dispersed by trypsin treatment with 1 ㎖ trypsin (Invitrogen) diluted to 0.25 % with PBS (-) for 50 sec at room temperature. To be sure cells are rounded up and detached from the surface, culture was checked with a microscope. As soon as cells were detached, 12 ㎖ medium containing 10% FBS was added to inhibit further trypsin activity that might damage cells. Detached cells reseeded into secondary cultures at a 1:12 split

ratio for a passage. If necessary, feed subconfluent cultures after 3 or 4 days by removing old medium and adding fresh medium. Cells at every other or the third passages were stored in the cell culture freezing medium-DMSO (Invitrogen) and kept in liquid nitrogen until use.

2. Cell proliferation assay

Subconfluent monolayer cultures were trypsinized, and collected in growth medium containing serum. The suspension was centrifuged for 5 min at 1500 rpm to pellet the cells in growth medium, and the number of cell was counted. Cells were diluted to 5×10^3 cells/ml and 100 μl of the suspension was added into each well of a flat-bottomed 96-well plate (NUNC™). During incubation at 37 °C in a humidified atmosphere with 5% CO_2, culture medium was replaced every other day. The number of cells in the proliferation was determined by addition of 20 μl of CellTiter 96® reagent (Promega, Madison, WI, USA), followed by incubation for 1 hr at 37℃ in a humidified, 5% CO_2 atmosphere. The CellTiter 96® reagent contains a novel tetrazolium compound, MTS. NADPH or NADH produced by dehydrogenase enzymes in metabolically active cells reduce MTS to colored formazan product. To measure the amount of formazan product generated by viable cells was measured at 490 nm with SpectraMax 340 (Molecular Devices, Sunnyvale, CA, USA).

3. Telomere length analysis

The terminal restriction fragment (TRF) length of rat hepatic epithelial cells was determined using the pulsed field gel electrophoresis (PFGE), and

the TRFs were then in-gel hybridized with telomeric probes. The methods described in previous reports[32,33,34] were modified in the following way.

Plug preparation: Cells grown at 80-90% confluency in a 100 mm tissue culture dish (NUNC™) were washed twice in ice-cold PBS and dispersed by trypsin treatment with 1 ml trypsin diluted to 0.25% with PBS for 50 sec at room temperature. After cells were detached, 12 ml of medium containing 10% FBS was added, followed by low-speed centrifugation at 1500 rpm for 5 min at 4℃. Pellets were resuspended at a concentration of 1×10^7 cells/500 μl in ice-cold PBS. The cell suspension was mixed with an equal volume (500 μl) of 2% certified™ low melt agarose (Bio-Rad, Hercules, CA, USA), pre-warmed at 37°C, to make plugs containing 1×10^6 cells/plug. The mixture was then cast into a 100 μl plug mold and cooled at 4 °C for 5 min. After casting, plugs were incubated in 25 ml of a lithium dodecyl sulfate (LDS) solution (1% LDS, 100 mM EDTA, pH 8.0, 10 mM Tris, pH 8.0) with constant agitation (55 rpm) at 37°C for 1 hr. The solution was replaced with fresh solution, and the aliquots were further incubated overnight. Plugs were then washed twice for 2 hr in 20% NDS (2 mM Tris, 6.8 mM N-laurylsarcosine, 127 mM EDTA, pH 9.5) and stored in 20% NDS at 4°C until use.

Pulsed field gel electrophoresis: DNA plugs were incubated in 500 μl TE buffer (10 mM Tris, 1 mM EDTA, pH 8.0) at room temperature for 1 hr, and it was repeated once again with fresh buffer. DNA plugs were then pre-incubated in 1× *Hin*f I restriction enzyme buffer (New England Biolabs,

Beverly, MA, USA) for 1 hr for two times. Plugs were cut with 4 mm long, which is two fifth of the plug. For *Hin*f I digestion, each plug was placed in 200 μl of 1× *Hin*f I buffer containing 30 units *Hin*f I (New England Biolabs), and incubated at 37 °C for 12 hr. After addition of 20 units *Hinf* I, the plugs were further incubated for 8 hr. Plugs were loaded into each well and covered with 1% Certified™ low melt agarose (Bio-Rad). DNA plugs on undergoing the same procedures without *Hin*f I were run in parallel to make sure that TRF signals are not in consequence of DNA degradation. Low range PFG marker was used as a molecular weight marker (New England Biolabs). Plugs were run on 1% pulsed field agarose (Bio-Rad) gel in 0.5× TBE. The gel was run using a CEFF-DR®III system (Bio-Rad) at a 6 V/cm at 14 °C for 16 hr, using ramped pulse times from 1 to 15 sec.

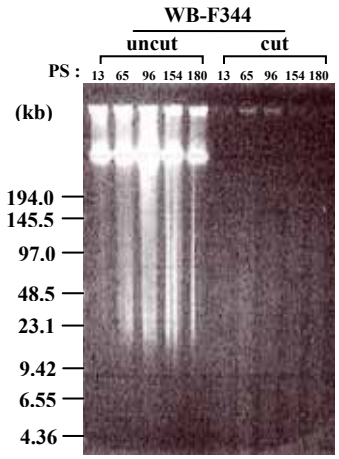

Figure 1. Ethidium bromide stained WB-F344 genomic DNA separated by PFGE.

To detect DNAs separated by PFGE, gel was stained with ethidium bromide

solution (1 μg/ml), and allowed it to stain for 10 min. After destaining with H_2O for 7 min, the gel was photographed under UV light (Fig. 1.).

In-gel hybridization: Gels were dried at 37 °C for 30 min. The DNA was denatured by soaking the gel for 30 min at room temperature in 500 ml denaturation solution (0.6 M NaCl, 0.5 M NaOH) with gentle agitation twice. The gel was rinsed briefly in deionized H_2O, and then neutralized by soaking for 30 min at room temperatue in 500 ml neutralization solution (1.5 M NaCl, 0.5 M Tris, pH 7.4) with constant agitation twice. After neutralization, the gel was placed in 100 ml pre-hybridization solution (5× SSC, 5× Denhardt's, 10 mM sodium phosphate) at 37°C for 1 hr. To make probe, 30 pmole of $d(CCCTAA)_4$ was incubated with 100 μCi [γ-^{32}P]ATP (Amersham, Buckinghamshire, England) and 15 units T4 polynucleotide kinase (TAKARA, Tokyo, Japan) for 1 hr at 37°C. Unincorporated labeled nucleotides from DNA labeling reaction were removed by using MicroSpin™ G-50 Columns (Amersham). The gel was hybridized with the probe in 5× SSC, 5× Denhardt's, 10 mM sodium phosphate at 37°C overnight. The gel was washed six times in 500 ml of 0.25× SSC at 37°C and placed on to a fresh piece of Saran Wrap. Gel was wrapped up and smooth out any air bubbles. The wrapped gel was placed in an X-ray film cassette with X-ray blue film for 13 hr at room temperature. Autoradiograph was scanned with luminescent image analysis system, LAS-1000 plus (Fujifilm, Tokyo, Japan). By using the Image Gauge Version 3.12 (Fujifilm), 1 × 25 grids were placed over a telomere lanes corresponding to the molecular size markers and quantitation was

performed. The optical density for each row was transferred to EXCEL (Microsoft). Molecular size for each row were determined by plotting the row number, 1~25, against the $\log_{10}$(molecular size) for the molecular size ladder. This allowed a molecular size to be calculated for each of 25 rows. The mean telomere length (MTL) of each lane was calculated with a formula, MTL = Σ(MW $\times$ OD)/ Σ(OD) where OD is the densitometer output and MW is the length of the DNA.[35]

4. γ-ionizing radiation

Subconfluent monolayer cultures were trypsinized, and collected at a concentration of 5×10^3 cells/100 μl in growth medium containing serum. Irradiation was carried out with a ^{137}Cs irradiator, Gammacell 3000 (MDS Nordion, Ottawa, Canada). Dose of γ-rays were 1, 2, 5, and 10 Gy. After irradiation, 100 μl of cells were plated onto each well of a flat-bottomed 96-well plate. Cells were incubated for 6 hr at 37 °C in a humidified atmosphere with 5% CO_2 and culture medium was replaced with fresh one. After 48 hr incubation at the same culture condition, the number of viable cells was determined by addition of 20 μl of CellTiter 96® reagent, followed by incubation for 1 hr at 37 ℃ in a humidified, 5% CO_2 atmosphere. To measure the amount of formazan product generated by viable cells was measured at 490 nm with SpectraMax 340.

5. Cloning of rPinX1

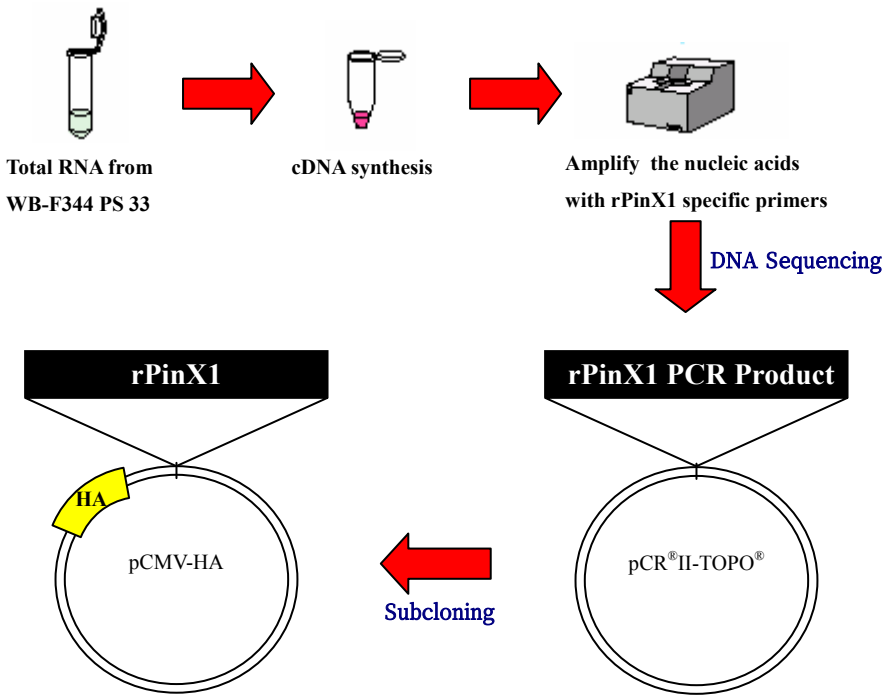

Figure 2. Scheme of rPinX1 cloning.

cDNA synthesis: To remove the genomic DNA completely, 2 μg of total RNA, isolated from WB-F344 cells at 33 passages, was treated with 5 units of DNase I (Takara) at 37 ℃ for 20 min. DNase I was inactivated by incubation with 25 nmol of EDTA, and by heat treatment at 65 ℃ for 20 min. For the first strand cDNA synthesis, a mixture, containing 120 pmol of random hexamers (Takara), 10 nmol dNTP and 1.7 μg of total RNA, was heated to 65 ℃ for 15 min and quick chilled on ice for 5 min. The contents of

the tube were collected by brief centrifugation, then 1× the first strand buffer (Invitrogen), 200 nmol DTT and 20 units of SUPERase·In™ RNase inhibitor (Ambion, Austin, TX, USA) were added. After incubation at 42 ℃ for 2 min, 200 units of Superscript™ II RNase H- reverse transcriptase (Invitrogen) were added. The cDNA synthesis was performed in 20 μl at 42 °C for 50 min and the reaction was inactivated by heating at 70 ℃ for 5 min. Two microgram of the cDNA was subjected to PCR with 2.5 units of Taq polymerase (Promega) at 94 °C/30 sec, 55 °C/30 sec and 72 °C/90 sec for 35 cycles. Nested PCR was performed to amplify the nucleic acids with same reverse primer. The primer sequences were as follows (1st forward primer: 5'-GAGTTGCGACAATGTCGATGCT-3', 2nd forward 5'-ACAATGTCGATGCTAGCGGA-3', reverse: 5'-CTATCTGGAAACTTTCTTCTTCTTCTTCAC-3'). Primer sequences were designed using the Primer Express™ (PE Applied Biosystems, Boston, MA, USA).

TOPO® cloning: The amplified PCR products were cloned into pCR®II-TOPO® vector (Invitrogen). The resulting PCR product ran on the 0.8% agarose gel and purified by using Gel Extraction Kit (Genenmed, Seoul, Korea) to 20 μl volume. TOPO® cloning reaction, containing 4 μl of fresh PCR product and 1 μl of pCR®II-TOPO® vector, was mixed gently and incubated for 20 min, followed by placing the mixture on ice. TOP 10 competent cell was thawed on ice, and then 2 μl of the TOPO® cloning reaction was added to a vial of competent cells and incubated on ice for 30 min. The cells were heat-shocked for 30 sec at 42 ℃ without shaking. Cells

were incubated on ice for 3 min. After 200 μl of room temperature SOC medium was added to cells, they were shaked horizontally with 200 rpm at 37 ℃ for 1 hr. Transformed *Escherichia coli* were grown on LB-agar (Invitrogen) plates containing 100 μg/ml ampicillin (AppliChem, Darmstadt, Germany) and 1.6 mg of X-gal (Amresco, Solon, OH, USA) overnight at 37 ℃. White colonies were selected in LB-agar plates containing 100 μg/ml ampicillin and plasmid DNA from these cells was prepared at 1.5 ml mini-scale. Correct direction was confirmed with digestion with 10 units of *Hin*d III.

Cloning of rPinX1 into pCMV-HA: To amplify the pCR®II-rPinX1, containing *Eco*R I restriction site, PCR was performed by using following primer (forward: 5'-AGGCCCGAATTCATATGTCGATGCTAGCGGAGCG-3', reverse: 5'-GCATGCTCGAGCGGCCGCCA-3'). For rPinX1 ΔN, +258-332 amino acids, PCR was performed by using following primer (forward: 5'-AGGCCCGAATTCATAGAGACCAAGTCGAGCTGCAG-3', reverse: 5'-GCATGCTCGAGCGGCCGCCA-3') and denaturing at 94 ℃ for 2 min, 34 cycles of amplification reaction (94 ℃/30 sec, 56 ℃/30 sec, 72 ℃/2 min), and final extention at 72 ℃ for 4 min with 1.25 units of Top-Pfu™ (Bio-online, Seoul, Korea) DNA polymerase for high fidelity synthesis. The PCR products were digested with 80 units of *Eco*R I and cloned into pCMV-HA plasmid (BD Biosiences Clontech, San Jose, CA, USA) digested with 120 units *Eco*R Ⅰ and dephospholyated with 100 units CIAP (Takara). The sequences of all

constructs were confirmed by DNA sequencing (Macrogen, Seoul, Korea).

6. Transfection

Exponentially growing NIH/3T3 cells were plated in a 6-well tissue culture plate at 4×10^5 cells/well and were grown overnight in a 5% CO_2 incubator at 37℃ to 50~60% confluency. One μg of DNA was pre-complexed with 3 μl of Plus™ Reagent (Invitrogen) in 100 μl of Opti-MEM® (Invitrogen), followed by incubation at room temperature for 15 min. In a second tube 2 μl of Lipofectamine™ reagent was diluted into 100 μl of Opti-MEM® (Invitrogen). Pre-complexed DNA and diluted Lipofectamine™ reagent were mixed together and incubated for 15 min at room temperature. While complexes were forming, cultured NIH/3T3 cells were washed once with 1 ml of Opti-MEM® (Invitrogen). For each transfection, 800 μl of Opti-MEM® (Invitrogen) was added to the tube containing the complexes and overlaid onto the rinsed cells. The culture plate was incubated for 3 hr at 37℃ in a CO_2 incubator. Medium was replaced with 2 ml of DMEM containing 10% FBS and incubated for 24~48 hr at the same culture condition. pIRES2-EGFP (BD Biosiences Clontech, San Jose, CA, USA) plasmid DNA was used to confirm the transfection efficiency of NIH/3T3 cells at the same condition (Fig. 3).

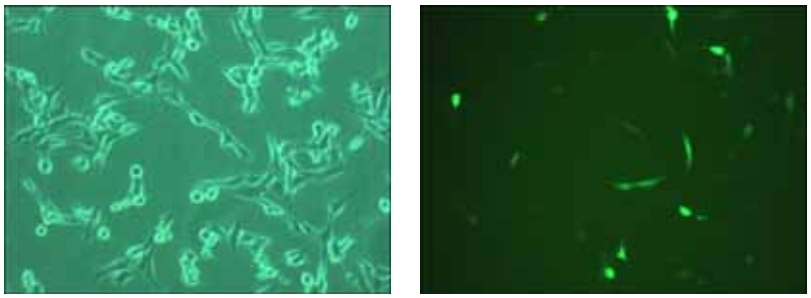

EGFP

Figure 3. Transfection efficiency of NIH/3T3. NIH/3T3 cells transfected with pIRES2-EGFP showed bright green fluorescence (left figure)

7. Immunofluorescence

4×10^4 cells, grown on sterile cover glass, were fixed in 4% formaldehyde/PBS for 20 min at room temperature, and then washed in cold PBS twice. Fixed cells were permeabilized with 0.2% Triton X-100/PBS on ice for 30 min, followed by washing with cold PBS twice. Non-specific sites were blocked by incubation at 2% bovine serum albumin (BSA) in PBS at 4℃ for 16 hr. Cells were incubated for 1 hr at room temperature with primary antibody, HA-probe (Y-11) rabbit polyclonal antibody (Santa Cruz Biotechnology, Santa Cruz, CA, USA) for HA tagged rPinX1 and fibrillarin antibody [38F3] – nucleolar marker (Abcam, Cambridge, UK) diluted with 2% BSA in PBS 1:200 and 1:500, respectively. The nucleolar marker fibrillarin is the human homologue of yeast Nop1p. Following three washes with 2% BSA in PBS for 5 min, the fluorochrome-conjugated secondary antibodys, Alexa Fluor® 488 $F(ab')_2$ fragment of goat anti-rabbit IgG (H+L) (Molecular Probes, Eugene, OR, USA) and Alexa Fluor® 594 $F(ab')_2$ fragment

of goat anti-mouse IgG (H+L) (Molecular Probes), were applied at the 1:500 dilutions in PBS plus 2% BSA and 6 μg/ml 4',6-diamidino-2-phenylindole (DAPI) (SIGMA). Secondary antibodies were removed and cells were washed with 2 ml of cold PBS for 5 min three times. Coverslip was mounted with a drop of mounting medium, ProLong® Gold antifade reagent (Molecular Probes), on a microscope slide and sealed with clear nail polish to prevent drying and movement under the microscope. After sealing, the slides ware stored upright in a covered slidebox at -20℃. Confocal microscopy was performed with a Radiance 2100™ (Bio-Rad) laser scanning system. All image acquisition controls were performed on the LaserSharp2000™ (Bio-Rad) operating software.

III. RESULTS

1. Growth rate of rat hepatic stem-like epithelial cells

LE/2, LE/6 and WB-F344 cells had been cultured for over 140 passages. A result of the proliferation assay, performed with LE/6 and WB-F344 at different passages was demonstrated in Figure 4. Under our culture conditions, LE/2 and LE/6 displayed a slow growth rate compared to WB-F344, but all these cells appeared to maintain a high proliferative rate without significant changes in the proliferation capacity, aging phenotype and cell crisis during *in vitro* aging.

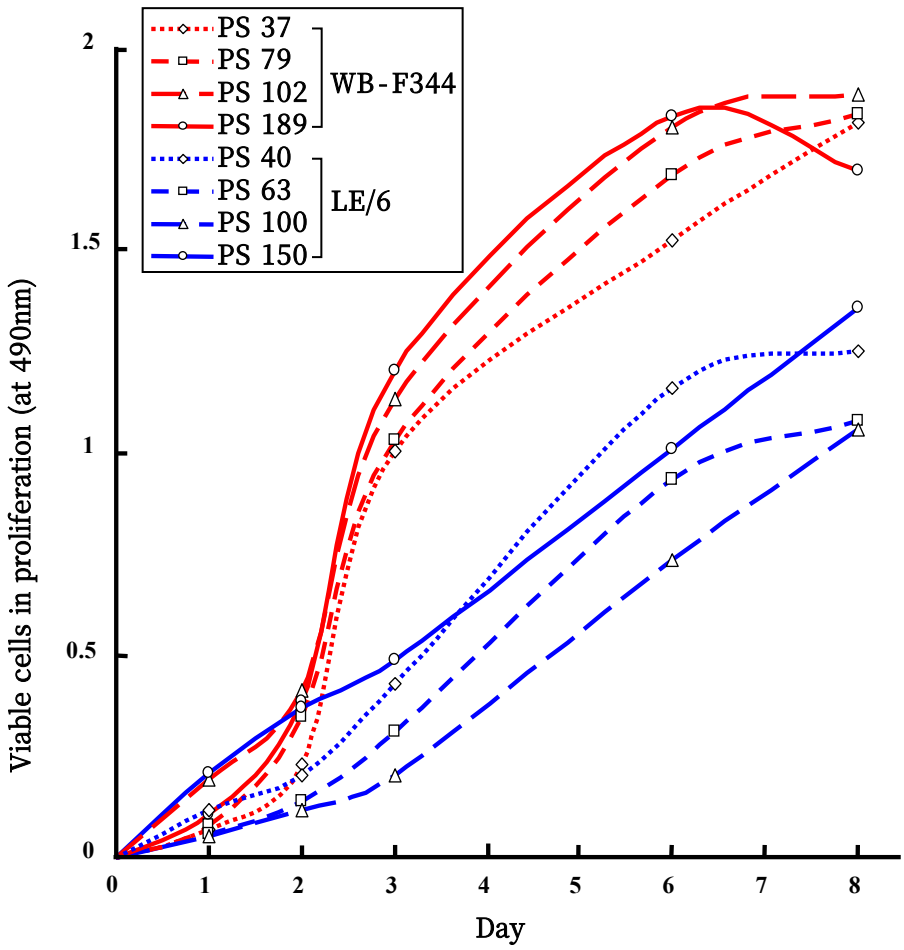

Figure 4. Proliferation of LE/6 and WB-F344 at different passages. Cell suspension (500 cells/100 µl) was incubated at 37 °C in a humidified atmosphere with 5% CO_2. Culture medium was replaced every 2 days. Viable cells in proliferation were measured at indicated days using CellTiter 96® reagent (Promega).

2. Telomere shortening during *in vitro* aging of rat hepatic stem-like epithelial cells

To investigate alteration of the telomere length during *in vitro* aging, the TRF length was determined using pulsed field gel electrophoresis followed by in-gel hybridization with telomere-specific probes, and the resulting hybridization signal was scanned using densitometry.

Telomere lengths of LE/2 were ranged in 10~150 kb (Fig. 5A). The imaging scan of autoradiography visualized signal shifts to a lower size as passages progressed, as shown in the right panel of Figure 5A. Cells at passage 35 showed multiple bands with strong signals in the range from 15 to 100 kb, which represented telomeres from different chromosomes. Cells at passages 75, 108, and 156 displayed a peak signal at near 20 kb, but the cells at passage 108 displayed strong signal at size < 20 kb compared to passage 75. The telomere shortening rate was ~50 bp per population doubling (pd) in overall, but it was slightly reduced in the late transition (108 ~156 passages) than the early period (35~75 passages).

The telomere length of LE/6 was detected in the range from 10 to 150 kb and appeared to be slightly longer than that of LE/2. The rate of telomere loss was ~50 bp/pd, similar to that of LE/2. The image scan of autoradiography showed telomere shortening with passages (Fig. 5B), but the telomere shortening was slightly reduced at the late passages. The peak signal of the passage 140 was shown at near 24 kb, which was similar to that of passage 102, and the signal at less than 24 kb was reduced at the passages 140.

WB-F344 possessed the telomere length in the range from 10 to 200 kb (Fig. 5C), which is apparently longer than that of LE cells. Telomere has progressively shortened from 13 to 96 passages, as telomerase activity has

gradually repressed. Telomere shortening continued until the passage 154, in which telomerase was reactivated, but at still low level. Further telomere shortening, however, did not appear at the last passage 180, where telomerase activity reached up to high level.

To make sure that TRF signals are not in consequence of DNA degradation, DNA plugs on undergoing the same procedures without *Hin*f I were run in parallel. Under our experimental conditions, DNA degradation has not been observed in all DNA plugs, and a representative result is shown in Figure 5C.

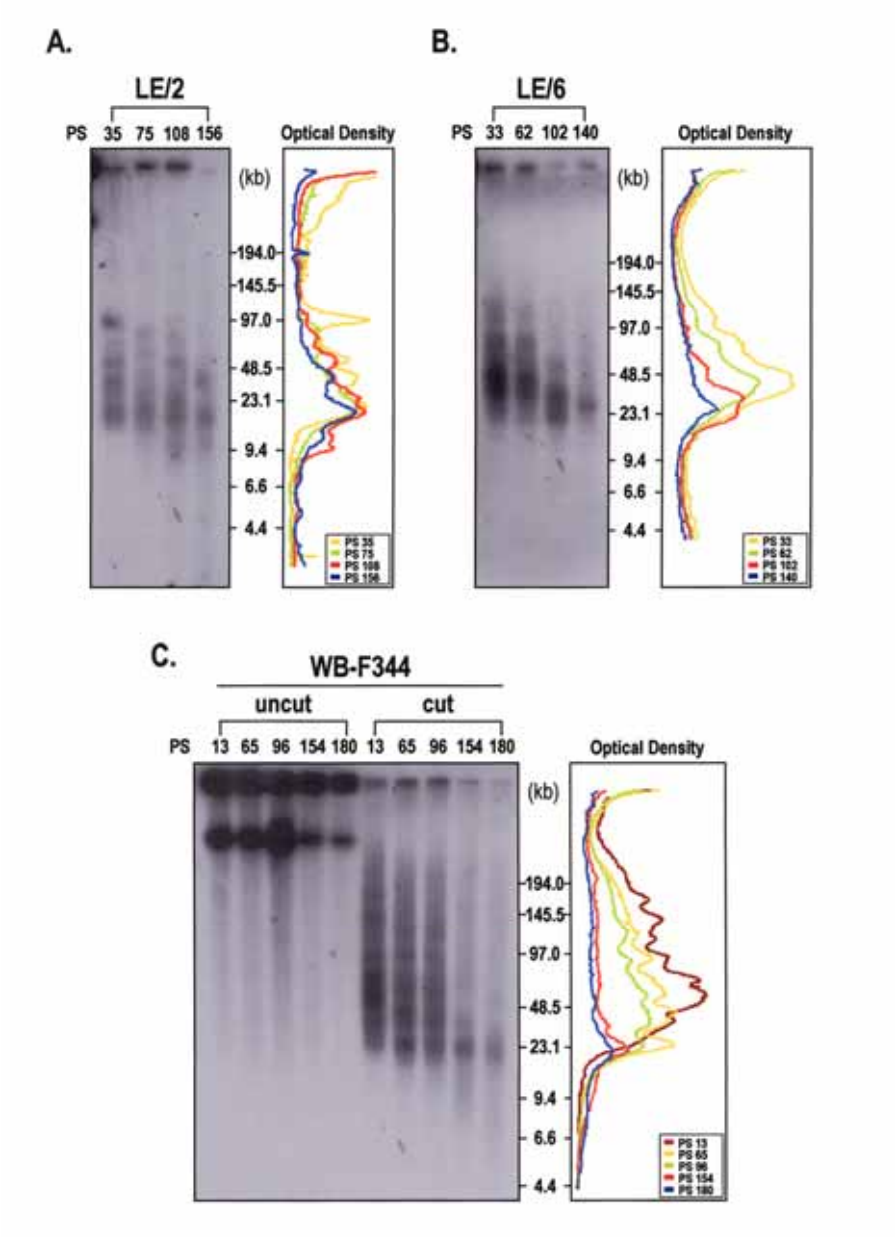

Figure 5. Telomere length of LE/2, LE/6 and WB-F344 during *in vitro* aging. Terminal restriction fragment (TRF) length of LE/2 (**A**), LE/6 (**B**) and

WB-F344 cells (**C**) was measured at different passages. DNAs embedded in agarose were digested with *Hin*f I and subjected to pulsed field gel electrophoresis. In WB-F344, DNA plugs digested with *Hin*f I were run in parallel with those of the DNA plugs on undergoing the same procedures without *Hin*f I digestion, denoted as cut and uncut, respectively. In-gel hybridization was followed with p^{32}-d$(CCCTAA)_4$. The gels exposed to X-ray films and their image scans are shown in left and right panel, respectively. Size markers are indicated between gel and image scans, and passages are indicated on the top of the gel figures.

3. Radiosensitivity in rat hepatic stem-like epithelial cells

To investigate the influence of ionizing radiation on the cells with various telomere length, the survival rate was examined after γ-irradiation at different passages. The survival rate of LE/2, LE/6 and WB-F344 cells that received various dosages of γ-ray is presented in Figure 6. There was no significant difference of sensitivity to the γ-irradiation according to different passages. LEs were relatively more resistant to the ionizing radiation compared to WB-F344, although LEs had a shorter telomere length than WB-F344.

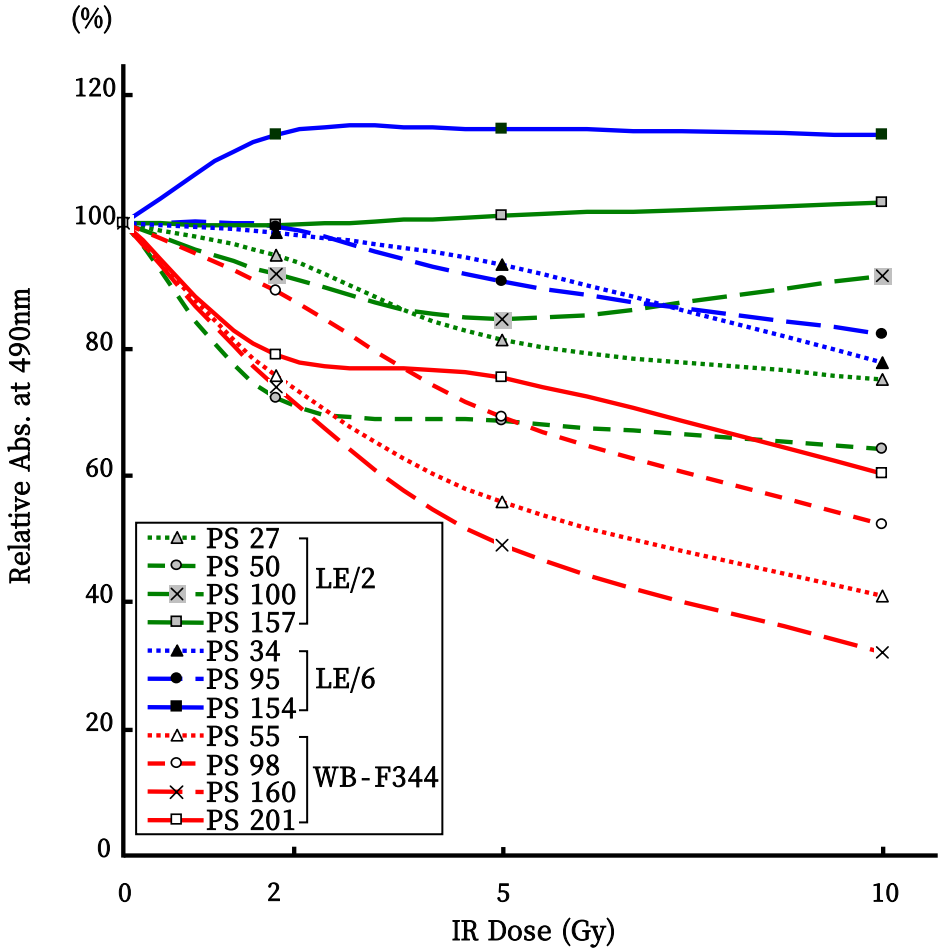

Figure 6. Radiosensitivity of LE/2, LE/6 and WB-F344 during *in vitro* aging. LE/2, LE/6 and WB-F344 cells irradiated with γ-rays over a wide range of dose (1~10 Gy). Relative radiosensitivity was measured by comparing non-irradiated cells with irradiated cells at each dose. Radiosensitivity was measured after 48 hr incubation of culture post-irradiation with CellTiter 96® reagent (Promega). This experiment was performed in four times and their mean value was presented.

4. Cloning of PinX1 from WB-F344 cell line

rPinX1 consisted of 331 amino acids containing the G-patch domain at the amino terminus. This domain had six highly conserved glycines (Fig. 7). An alignment of PinX1 was performed by using Vector NT I 7.1 (Invitrogen) and slightly refined manually (Fig. 8). Sequence alignment tool, ALIGN (http://www2.igh.cnrs.fr/bin/align-guess.cgi) was used to know sequence similarity. rPinX1 was identical to hPinX1 about 69.5% in multiple sequence alignment and mPinX1 with 91% (Fig. 8). G-patch was also conserved at the rPinX1, like hPinX1 (Fig. 8). The N-terminus of PinX1 was highly conserved among human, rat and mouse, while the C-terminus was quite different (Fig. 8). To study the functional region of rPinX1, rPinX1 Δ N, N-terminal deleted form of rPinX1, was also constructed by cloning.

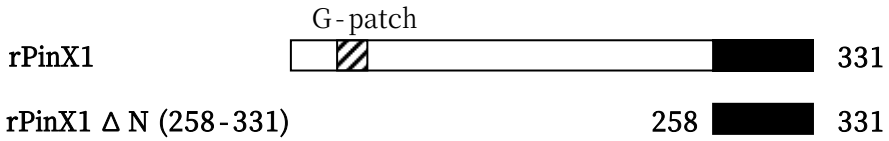

Figure 7. Domain structure of rPinX1

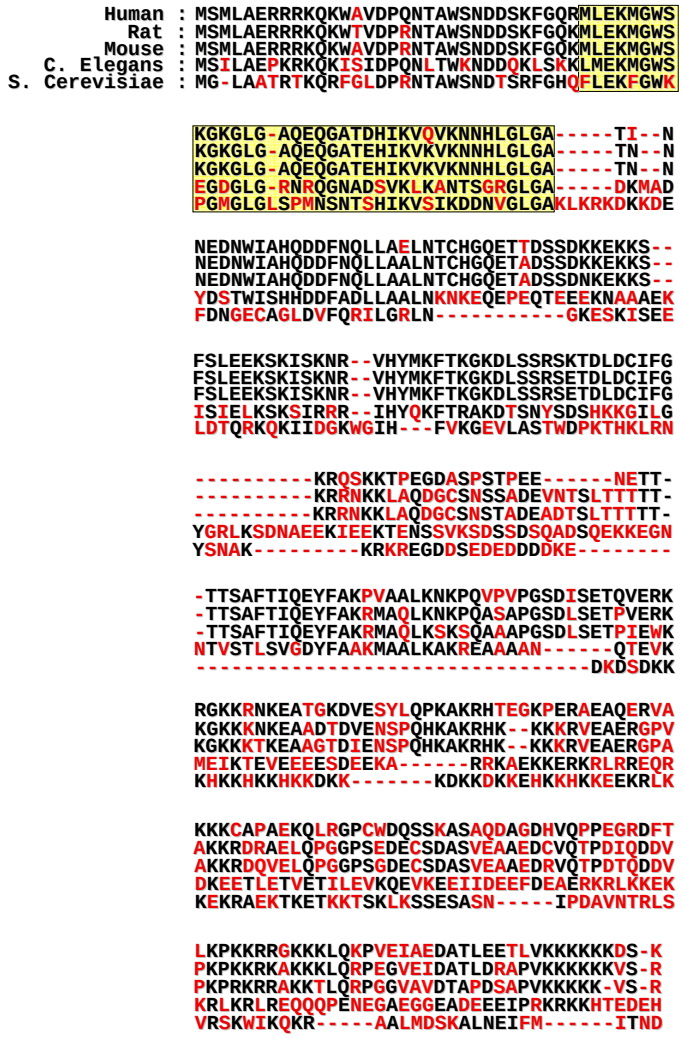

Figure 8. Multiple sequence alignment of PinX1s. In the result of sequence alignment among human (*Homo sapiens*), rat (*Rattus norvegicus*) and mouse (*Mus musculus*), rat encoded a protein about 69.5% identical to the human PinX1p. In case of *Caenorhabditis elegans* and *Saccharomyces cerevisiae*, about 31.1% and 27% similarity was confirmed, respectively. Black letters are identical or conserved residues. G-patch was represented as yellow background.

5. Subcellular localization of rPinX1

To investigate the subcellular localization of rPinX1 in a rodent cell, rPinX1-HA construct and its N-terminal deletion mutant, rPinX1Δ N were transiently expressed in NIH/3T3, mouse transformed fibroblast, and assayed for subcellular localization. Fibrillarin was used as a marker for nucleolus. rPinX1 was colocalized with fibrillarin in nucleolus (Fig. 9B). However, rPinX1 Δ N appeared to be present in both nucleus and cytoplasm (Fig. 9C), without showing colocalization with fibrillarin.

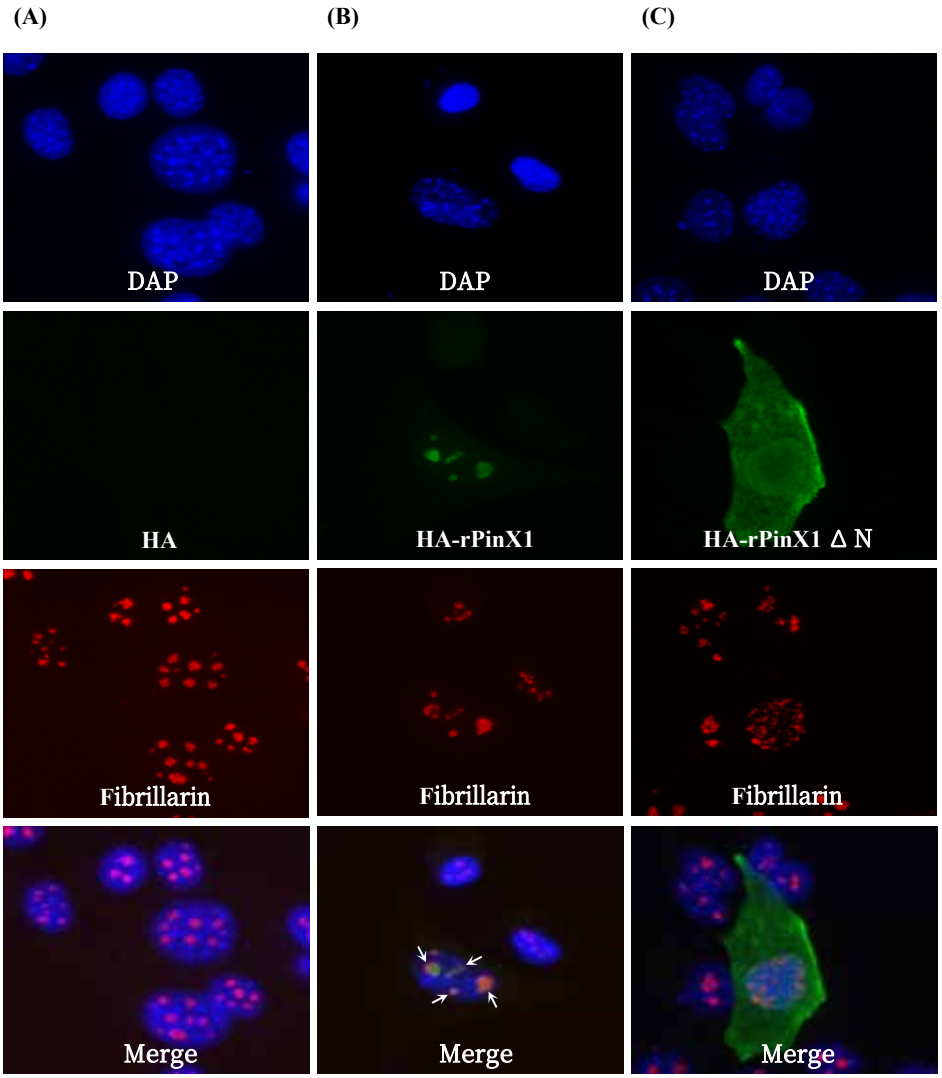

Figure 9. Intracellular localization of transiently expressed rat PinX1 protein in NIH/3T3. NIH/3T3 cells expressing HA-rPinX1 were fixed, stained for a nucleolar marker and visualized simultaneously for HA (rPinX1) and Alexa Fluor® 594 (nucleoli). Fluorescence localization of HA in NIH/3T3

cells expressing HA-rPinX1 or HA-rPinX1 ΔN, but not in cells expressing HA alone. (**A**) NIH/3T3, transfected with pCMV-HA, used as a control. (**B**) Ectopic HA-rat PinX1 fusion protein (green) in NIH/3T3 cell line shows a nucleolar concentration pattern, arrowed (purple). (**C**) NIH/3T3, transiently expressed HA-rat PinX1 ΔN, showed even distribution to both nucleus (green) and cytoplasm (green). Cells were treated with an anti-fibrillarin antibody to detect the nucleolar protein fibrillarin (red). Nucleus, stained with DAPI, was presented as blue. Cells were observed at ×2000 magnification.

IV. DISCUSSION

LE/2, LE/6 and WB-F344 are hepatic stem-like epithelial cells and their morphological and biochemical properties have been previously characterized.[1,2,36,37,38,39] LE/2 and LE/6 cells, isolated from Sprague-Dawley rat fed CDE diet (choline-deficient diet containing 0.1% ethionine) for 2 and 6 weeks, respectively, were known to possess similar phenotypical and biochemical features. WB-F344, isolated from the liver of an adult male Fisher-344 rat, is known to have phenotypic properties similar to oval cells, like LE/2 and LE/6.[2,40,41] In this study, these cells were cultured for over 140 passages to investigate the telomere maintenance during *in vitro* cellular aging. All these cells appeared to grow without significant changes in proliferative capacity and aging phenotype during *in vitro* aging.

LE/2 and LE/6 cells displayed a similar pattern of the telomere shortening. Telomere length of LE cells shortened with a rate of telomere loss of ~50 bp/pd, which is comparable to the result observed in human telomerase negative cells (50~100 bp/cell division).[13]

In our previous report,[42] the telomerase activity of LE/2 and LE/6 declined from the early to intermediate passages and progressively increased from the intermediate to late passages. Comparing the telomere length and telomerase activity, progressive telomere shortening seems to be occurred due to a low level of the telomerase activity of LE cells. The telomere shortening rate of LEs appeared to be slower in the late passages, in which telomerase activity inclined, than in the early passages, although its difference was small. These results may be explained by the following that the telomerase activity

in LE cells is not strong enough to prevent telomere erosion during passages, but the reactivated telomerase in late passages seems to enable to reduce the telomere decay rate.

WB-F344 was also found to possess a strong telomerase activity in our previous result,[42] particularly at early and late passages, with a high proliferation rate, which appeared to be comparable to human cancer cells. The high proliferative capacity of WB-F344 is likely related to the strong telomerase activity.[43] The telomerase regulation and progressive telomere shortening during *in vitro* aging showed patterns similar to those of LE lines, and this result is consistent with a previous report.[44] An apparent decrease of telomere length was found in the transition from passage 96 to 154, in which telomerase activity was being induced but still low in the level, and no further reduction appeared at the passage 180. These results suggest that the telomerase activity in the period from 96 to 154 is not yet strong enough to prevent telomere loss, while the strong telomerase at the passage 180 maintains the telomeres without further telomere erosion. Taken together, the weak telomerase expression of LEs and WB-F344 at the early passages does not seem to prevent telomere shortening, and telomerase reactivation at late passages, especially of WB-F344 cell, maintain telomeres without further telomere decay.

Telomere dysfunction impairs DNA repair and enhances sensitivity to ionizing radiation,[45] and short telomeres of mammalian cells result in organismal hypersensitivity to ionizing radiation.[46] In this study, all of LE/2, LE/6 and WB-F344 showed no significant difference in radiosensitivity according to the different passages. The telomere length might not be critically shortened to induce chromosomal instability at even late passages,

and there is a possibility that LEs and WB-F344 cells might possess mechanism(s) to DNA repairs and intact cell cycle pathways, which contribute to the chromosomal stability.

PinX1 was reported as a telomerase inhibitor in human cells. Overexpression of hPinX1 and its TID, interact with TRF1, inhibited telomerase activity, shortened telomeres and induced crisis with TID being more potent than the full length protein.[28] hPinX1 mainly localize at the nucleolus and colocalize with Pin2 in the nucleus with speckle pattern.[28] To determine the functional region of rPinX1 involved in subcellular localization, two plasmid constructs, rPinX1 and rPinX1 Δ N, were prepared and were transiently overexpressed in NIH/3T3. rPinX1 was observed at the nucleolus in the NIH/3T3. Contrary to rPinX1, rPinX1 Δ N, without G-patch region, was localized to nucleus and cytoplasm with no speckle pattern. It is speculated that G-patch domain could involve in nucleolar localization of rPinX1. Considering that PinX1 binds hTERT/hTR complex *in vivo*[29], localization of rPinX1 in nucleolus might have less chance to associate telomerase that is mainly localized in nucleus. It might be difficult for rPinX1 to inhibit the activity of telomerase in the nucleus.

In conclusion, telomerase activity was presented and contributed to the regulation of telomere length in LE/2, LE/6 and WB-F344 cells. We confirmed the nucleolar localization of transiently overexpressed rPinX1 in NIH/3T3 cells. On the basis of these observations, subcellular localization of PinX1 may be important on the regulation of the telomerase activity in rat hepatic stem-like epithelial cells.

V. CONCLUSION

In summary, progressive telomere shortening was shown in the LEs and WB-F344 cells during *in vitro* aging. At the late passage of these cells, their mean telomere lengths were shorter than those of at the early passage. However, there was no relation between telomere shortening and radiosensitivity. The subsequent telomere shortening had not concerned with radiosensitivity in the LEs and WB-F344 cells. This result suggests that the telomere length in these cells might not be critically shortened to induce chromosomal instability. rPinX1 sequence, containing G-patch, was similar with hPinX1. rPinX1 was localized at nucleolus and its N-terminus deleted form, rPinX1 Δ N, was located in nucleus and cytoplasm. Accordingly, rPinX1 Δ N, located at the nucleus, may have more chances to associate with telomerase, present in nucleus, compared to rPinX1. In rat hepatic stem-like epithelial cells, constantly express rPinX1 gene during *in vitro* aging, the localization of rPinX1 might be important to regulate telomerase activity. This study would provide a better understanding of PinX1 mechanisms related to telomere maintenance in the rodent cells.

REFERENCES

1. Yaswen P, Hayner NT, Fausto N. Isolation of oval cells by centrifugal elutriation and comparison with other cell types purified from normal and preneoplastic livers. Cancer Res. 1984;44:324-331.
2. Tsao MS, Smith JD, Nelson KG, Grisham JW. A diploid epithelial cell line from normal adult rat liver with phenotypic properties of 'oval' cells. Exp. Cell Res. 1984;154:38-52.29.
3. Grisham JW, Coleman WB, Smith GJ. Isolation, culture, and transplantation of rat hepatocytic precursor (stem-like) cells. Proc. Soc. Exp. Biol. Med. 1993;204:270-279.
4. Germain L, Goyette R, Marceau N. Differential cytokeratin and alpha-fetoprotein expression in morphologically distinct epithelial cells emerging at the early stage of rat hepatocarcinogenesis. Cancer Res. 1985;45:673-681.
5. Hixson DC, Faris RA, Thompson NL. An antigenic portrait of the liver during carcinogenesis. Pathobiology 1990;58:65-77.
6. Blackburn EH. Switching and signaling at the telomere. Cell 2001;106:661-673.
7. de Lange T. Protection of mammalian telomeres. Oncogene 2002;21:532-540.
8. Chan SW, Blackburn EH. New ways not to make ends meet: telomerase, DNA damage proteins and heterochromatin. Oncogene 2002;21:553-563.
9. Feng J, Funk WD, Wang SS, Weinrich SL, Avilion AA, Chiu CP, et al. The RNA component of human telomerase. Science 1995;269:1236-1241.
10. Nakamura TM, Cech TR. Reversing time: origin of telomerase. Cell

1998;92:587-590.

11. Ford LP, Wright WE, Shay JW. A model for heterogeneous nuclear ribonucleoproteins in telomere and telomerase regulation. Oncogene 2002;21:580-583.
12. Allsopp RC, Vaziri H, Patterson C, Goldstein S, Younglai EV, Futcher AB, et al. Telomere length predicts replicative capacity of human fibroblasts. Proc. Natl. Acad. Sci. USA. 1992;89:10114-10118.
13. Counter CM, Avilion AA, LeFeuvre CE, Stewart NG, Greider CW, Harley CB, et al. Telomere shortening associated with chromosome instability is arrested in immortal cells which express telomerase activity. EMBO. J. 1992;11:1921-1929.
14. Harley CB, Futcher AB, Greider CW. Telomeres shorten during ageing of human fibroblasts. Nature 1990;345:458-460.
15. Kim NW, Piatyszek MA, Prowse KR, Harley CB, West MD, Ho PL, et al. Specific association of human telomerase activity with immortal cells and cancer. Science 1994;266:2011-2015.
16. Shay JW, Bacchetti S. A survey of telomerase activity in human cancer. Eur. J. Cancer 1997;33:787-791.
17. Kipling D, Cooke HJ. Hypervariable ultra-long telomeres in mice. Nature 1990;347:400-402.
18. Prowse KR, Avilion AA, Greider CW. Identification of a nonprocessive telomerase activity from mouse cells. Proc. Natl. Acad. Sci. USA. 1993;90:1493-1497.
19. Chadeneau C, Siegel P, Harley CB, Muller WJ, Bacchetti S. Telomerase activity in normal and malignant murine tissues. Oncogene 1995;11:893-898.

20. Broccoli D, Godley LA, Donehower LA, Varmus HE, de Lange T. Telomerase activation in mouse mammary tumors: lack of detectable telomere shortening and evidence for regulation of telomerase RNA with cell proliferation. Mol. Cell Biol. 1996;16:3765-3772.
21. Newbold RF. The significance of telomerase activation and cellular immortalization in human cancer. Mutagenesis 2002;17:539-550.
22. Goytisolo FA, Samper E, Martin-Caballero J, Finnon P, Herrera E, Flores JM, et al. Short telomeres result in organismal hypersensitivity to ionizing radiation in mammals. J. Exp. Med. 2000;192:1625-1636
23. Wong KK, Chang S, Weller SR, Ganesau S, Chaudhuri J, Zhu C, et al. Telomere dysfunction impairs DNA repair and enhances sensitivity to ionizing radiation. Nat. Genet. 2000;26:85-88
24. Metcalfe JA, Parkhill J, Campbell L, Stacey M, Biggs P, Byrd PJ, et al. Accelerated telomere shortening in ataxia telangiectasia. Nat. Genet. 1996;13:350-353
25. Hande P, Slijepcevic P, Silver A, Bouffler S, van Buul P, Bryant P, et al. Elongated telomeres in scid mice. Genomics 1999; 56:221-223
26. Samper E, Goytisolo FA, Slijepcevic P, van Buul PP, Blasco MA. Mammalian Ku86 protein prevents telomeric fusions independently of the length of TTAGGG repeats and the G-strand overhang. EMBO Rep. 2000;1:244-252
27. Liao C, Zhao M, Song H, Uchida K, Yokoyama KK, Li T, Identification of the gene for a novel liver-related putative tumor suppressor at a high-frequency loss of heterozygosity region of chromosome 8p23 in human hepatocellular carcinoma. Hepatology 2000;32:721-727.
28. Zhou XZ, Lu KP. The Pin2/TRF1-interacting protein PinX1 is a potent

telomerase inhibitor. Cell 2001;107:347-359.

29. Banik SS, Counter CM. Characterization of interactions between PinX1 and human telomerase subunits hTERT and hTR. J Biol Chem. In press 2004.
30. Lin J, lackburn EH. Nucleolar protein PinX1p regulates telomerase by sequestering its protein catalytic subunit in an inactive complex lacking telomerase RNA.Genes Dev. 2004;18:387-396.
31. Guglielmi B, Werner M. The yeast homolog of human PinX1 is involved in rRNA and small nucleolar RNA maturation, not in telomere elongation inhibition. J Biol Chem. 2002;277:35712-35719.
32. Dionne I, Wellinger RJ. Cell cycle-regulated generation of single-stranded G-rich DNA in the absence of telomerase. Proc. Natl. Acad. Sci. USA. 1996;93:13902-13907.
33. Hemann MT, Greider CW. G-strand overhangs on telomeres in telomerase-deficient mouse cells. Nucleic Acids Res. 1999;27:3964-3969.
34. Hemann MT, Greider CW, Wild-derived inbred mouse strains have short telomeres. Nucleic Acids Res. 2000;28:4474-4478.
35. Kruk PA, Rampino NJ, Bohr VA. DNA damage and repair in telomeres: relation to aging. Proc Natl Acad Sci U S A. 1995;92:258-262.
36. Hayner NT, Braun L, Yaswen P, Brooks M, Fausto N. Isozyme profiles of oval cells, parenchymal cells, and biliary cells isolated by centrifugal elutriation from normal and preneoplastic livers. Cancer Res. 1984;44:332-338.
37. Petropoulos CJ, Yaswen P, Panzica M, Fausto N. Cell lineages in liver carcinogenesis: possible clues from studies of the distribution of alpha-fetoprotein RNA sequences in cell populations isolated from normal,

regenerating, and preneoplastic rat livers. Cancer Res. 1985;45:5762-5768.

38. Yaswen P, Thompson NL, Fausto N. Oncodevelopmental expression of rat placental alkaline phosphatase. Detection in oval cells during liver carcinogenesis. Am. J. Pathol. 1985;121:505-513.
39. Hooth MJ, Coleman WB, Presnell SC, Borchert KM, Grisham JW, Smith GJ. Spontaneous neoplastic transformation of WB-F344 rat liver epithelial cells. Am. J. Pathol. 1998;153:1913-1921.
40. Fausto N, Thompson NL, Braun L. Purification and culture of oval cells from rat liver, in: T.G. Pretlow, T.P. Pretlow (Ed.), In Cell Separation Methods and Selected Applications (FL): Academic Press; 1987.
41. Kaufmann WK, Behe CL, Golubovskaya VM, Byrd LL, Albright CD, Borchet KM, et al. Aberrant cell cycle checkpoint function in transformed hepatocytes and WB-F344 hepatic epithelial stem-like cells. Carcinogenesis 2001;22:1257-1269.
42. Oh BK, Lee CH, Park C, Park YN. Telomerase regulation and progressive telomere shortening of rat hepatic stem-like epithelial cells during in vitro aging. Exp Cell Res. 2004;298:445-454.
43. Holt SE, Wright WE, Shay JW. Regulation of telomerase activity in immortal cell lines. Mol. Cell. Biol. 1996;16:2932-2939.
44. Golubovskaya VM, Filatov LV, Behe CI, Presnell SC, Hooth MJ, Smith GJ, et al. Telomere shortening, telomerase expression, and chromosome instability in rat hepatic epithelial stem-like cells. Mol. Carcinog. 1999;24:209-217.
45. Wong KK, Chang S, Weiler SR, Ganesan S, Chaudhuri J, Zhu C, et al. Telomere dysfunction impairs DNA repair and enhances sensitivity to ionizing radiation. Nat. Genet. 2000;26:85-88.

46. Goytisolo FA, Samper E, Martin-Caballero J, Finnon P, Herrera E, Flores JM, et al. Short telomeres result in organismal hypersensitivity to ionizing radiation in mammals. J. Exp. Med. 2000;192:1625-1636.

Abstract (in Korean)

랫 상피 간세포에서 계속적으로 일어나는 telomere 길이 감소와 랫 PinX1의 세포 내 위치

<지도교수 박영년>

연세대학교 대학원 의과학과

이찬희

랫의 상피 간세포인 LE/2, LE/6 와 WB-F344 세포는 간암 발생 초기 단계에서 관찰되는 타원 세포와 표현형에 있어서 많은 공통점이 있다. Telomerase는 telomere의 3'말단에 TTAGGG 반복 서열을 붙여 줌으로서 세포분열에 따른 telomere 길이 감소를 막아주는 기능을 하므로 세포 노화를 극복해 무한 분열을 하는 세포들에서 telomerase 활성은 중요하다. 선행 연구에서 LE/2,LE/6 와 WB-F344 세포의 telomerase 활성이 초반 계대에서 중반 계대까지 감소하다가 후반 계대로 진행됨에 따라 점진적으로 증가함을 알 수 있었다. 본 연구에서 이들 세포의 telomere 길이 변화를 측정해 본 결과, 계대를 거치는 동안 계속적인 telomere 길이 감소 현상을 보였고, 140 계대 이상을 거치는 동안 분명한 노화 형질을 보이지

않았다. Telomere 길이와 telomerase 활성의 상관관계를 보았을 때, 후반 계대의 세포에서 telomerase 활성이 증가함에 따라 telomere 길이 감소가 둔화되었으므로 이들 세포에서 telomerase는 telomere 길이 조절에 관여한다고 볼 수 있겠다. 짧은 telomere를 갖는 세포는 전리 방사선에 매우 민감하다고 알려져 있다. 따라서 랫 세포 내 짧은 길이의 telomere가 전리 방사선 조사에 대한 민감도를 증가시키는가를 알아보기 위해서 각기 다른 계대의 LE/2,LE/6 와 WB-F344 세포에 감마선을 조사하였다. 이들 세포의 각기 다른 계대에 있어서 감마선에 대한 민감도 차이는 볼 수 없었다. 최근에 유력한 telomerase 억제 물질로 밝혀진 PinX1의 특성을 알아보고자, WB-F344 세포주로부터 rPinX1을 클론하여 NIH/3T3 세포에 과발현시켜 공초점 현미경 관찰 결과 rPinX1이 핵인에 위치함을 보았고, rPinX1의 아미노 말단 서열을 절단한 형태인 rPinX1 Δ N은 핵과 세포질에 위치하고 있음을 보았다.

결론적으로, LE/2,LE/6 와 WB-F344 세포들의 telomere는 telomerase에 의해 조절되고, NIH/3T3 세포에서 일시적으로 과 발현된 rPinX1이 핵인에 위치했고, 이는 rPinX1의 세포 내 위치가 telomerase 활성 억제 기능에 영향을 미칠 가능성을 제시하고 있다.

핵심 되는 말 : 랫 상피 간세포, telomerase, telomere, PinX1, 감마선 조사